Groff, D.V., et al., 2023, Kill dates from re-exposed black mosses constrain past glacier advances in the northern Antarctic Peninsula: Geology, https://doi.org/10.1130/G50314.1

Supplemental Material
Kill dates from re-exposed black mosses constrain past glacier advances in the northern Antarctic Peninsula

Dulcinea V. Groff[1,2], David W. Beilman[3], Zicheng Yu[4,5,2], Derek Ford[3], Zhengyu Xia[2,4]

SUPPLEMENTAL METHODS

We established three strict collection criteria to maximize the quality of black moss samples for ^{14}C measurement: mosses must be found *in situ*, show no evidence of regrowth, and tops must be present. First, black mosses classified as *in-situ* were found in a bedrock crevice, sheltered by surrounding rock. Additionally, the sampling areas were void of lichens indicating very recent deglaciation (Smith, 1982). Black moss samples that appeared to be transported through erosional and sedimentary processes and not in original growth position with erect stems were not classified as *in situ*. Second, mosses were inspected in the field for potential "moss regrowth", i.e. green moss growing upon black moss either by regeneration (La Farge et al., 2013) or growth of a new propagule using the black moss as substrate, which would contaminate kill dates with young carbon. Third, because glacier advances and recessions could damage the most recent growth at acrocarpous moss apices, we determined if moss tops are intact or "tops present" in the field and in the lab. If part of the moss other than the top is ^{14}C dated, then the date would not reflect the kill date of the moss. Collected mosses were frozen below -20°C within eight hours of collection until processed.

Sample pretreatment of black mosses included acid-base-acid (1N HCl and 1N NaOH, 75°C) prior to combustion, and accelerated mass spectrometry ^{14}C dating were performed at the University of California Irvine Keck Laboratory and the Center for Accelerator Mass Spectrometry within Lawrence Livermore National Laboratory. We applied the SHCal20 curve (Hogg et al., 2020) and summarized the temporal density of all samples using sum probability distribution in Calib v.8.2 (Stuiver and Reimer, 1993). We compared the sum probability distribution of all samples with two simulated sum probability distributions to test the sensitivity to the calibration curve. We selected n=67 evenly spaced cal BP / calendar ages (every 22 years) from 1500 to 0 cal yr BP and extracted the ^{14}C year from the SHCal20 curve. The ^{14}C ages were then calibrated using SHCal20 and the sum probability distribution calculated. (Supplemental Fig. S2).

We calibrated previously published proxies for penguin colony abandonment, radiocarbon ages of penguin remains (i.e. feather, bone, eggshell membrane) or penguin prey (i.e. squid beak) for n=158 samples less than 2,050 years ^{14}C age found in Appendix B (Emslie, 1995, 2001; Emslie et al., 1998, 2003, 2011, 2013, 2018, 2020; Kalvakaalva

et al., 2020). We applied a marine reservoir correction (Δ R) of 700 ± 50 years (Emslie, 2001) and Δ R = 802 ± 97 years calculated using published ages found in the 14CHRONO Marine20 Reservoir database (Reimer and Reimer, 2001). For this we averaged reported Δ R values 813 ± 40 and 873 ± 39 (Berkman and Forman, 1996), and 669 ± 50 (Björck et al., 1991). Our sensitivity analysis of the two ΔR reservoir age corrections, revealed negligible differences.

The ^{10}Be ages of select samples (n=9) less than 1500 years old from Kaplan et al., (2020) collected from moraines, erratics, supraglacial debris, and ice edges largely coincide with peaks in kill dates. ^{10}Be ages reported in Kaplan et al. 2020 are relative to the year collected. For a more accurate comparison with black moss radiocarbon ages, which were relative to AD 1950, we subtracted 64 years (collection years was AD 2014 in Kaplan et al., (2020)) from each ^{10}Be age.

Table S1. Samples of black mosses radiocarbon dated from this study, and other published sources (a=this study, b=Hall, 2007; c=Hall, 2010; d=Guglielmin et al., 2016; e=Yu et al., 2016. We applied the SHCal20 curve (Hogg et al., 2020) to all black moss dates in OxCal (version 4.4), except a modern sample indicated by *, reported in Fraction Modern (FM). SD=Standard Deviation. Superscripts for collection year: 1=2020; 2=2019; 3=2014; 4=2011; 5=2009; 6=2006;

No.	Source	Lab_ID	ID	Region	Latitude	Longitude	$\delta^{13}C$ (‰)	^{14}C Date ± SD	Med. Age (cal yr BP)	2-σ range (cal yr BP)
1	a	CAMS-184078	BON_DM21	Anvers Island[2]	-64.7769	-64.0422	-26.0	690 ± 20	600	558-660
2	a	CAMS-184075	BON_DM10B	Anvers Island[2]	-64.7773	-64.0414	-25.8	830 ± 25	703	670-735
3	a	CAMS-184079	BON_DM24	Anvers Island[2]	-64.7769	-64.0413	-25.5	800 ± 35	694	576-736
4	a	CAMS-184077	BON_DM15	Anvers Island[2]	-64.7771	-64.0413	-23.8	630 ± 30	604	535-647
5	a	CAMS-184076	BON_DM14	Anvers Island[2]	-64.7771	-64.0411	-24.4	740 ± 30	645	562-680
6	a	CAMS-184082	BON_DM32B	Anvers Island[2]	-64.7772	-64.0400	-27.7	900 ± 25	757	685-896
7	a	CAMS-184080	BON_DM25	Anvers Island[2]	-64.7764	-64.0394	-25.7	965 ± 25	848	769-917
8	a	CAMS-184081	BON_DM28	Anvers Island[2]	-64.7764	-64.0391	-25.3	920 ± 35	778	688-905
9	a	CAMS-184083	GAM_DM1	Anvers Island[2]	-64.774	-64.0514	-25.0	1450 ± 30	1309	1276-1361
10	a	CAMS-184085	GAM_DM6	Anvers Island[2]	-64.7743	-64.0474	-22.2	770 ± 50	668	561-736
11	a	CAMS-184086	GAM_DM11	Anvers Island[2]	-64.773	-64.0473	-26.2	1025 ± 35	863	797-958
12	a	CAMS-184087	GAM_DM16	Anvers Island[2]	-64.7746	-64.0469	-25.0	980 ± 30	852	771-924
13	a	UCIAMS-240437	GAM_DM10	Anvers Island[2]	-64.7736	-64.0462	-24.9	885 ± 15	748	689-790
14	a	UCIAMS-240432	GAM_DM21	Anvers Island[2]	-64.7737	-64.0448	-25.5	855 ± 15	709	677-762
15	a	UCIAMS-240431	GAM_DM23	Anvers Island[2]	-64.7734	-64.0438	-25.9	835 ± 15	702	676-731
16.	a	CAMS-184084	GAM_DM2	Anvers Island[2]	-64.7744	-64.0505	-25.5	1005 ± 30	856	796-928
17.	a	UCIAMS-240435	GAM_DM38	Anvers Island[2]	-64.7725	-64.0404	-24.9	875 ± 15	737	682-787
18.	a	UCIAMS-240436	GAM_DM30	Anvers Island[2]	-64.7722	-64.0384	-24.8	870 ± 15	732	680-770
19.	a	UCIAMS-240433	GAM_DM32	Anvers Island[2]	-64.7721	-64.0366	-25.2	910 ± 15	762	732-795
20.	a	UCIAMS-240434	GAM_DM33	Anvers Island[2]	-64.7722	-64.0353	-25.5	920 ± 15	771	732-878
21.	a	UCIAMS-240438	GAM_DM2	Anvers Island[1]	-64.7721	-64.0347	-25.7	975 ± 15	859	793-913
22.	a	UCIAMS-240426	RAS_DM1	Cape Rasmussen[1]	-65.2471	-64.0811	-23.3	1495 ± 15	1335	1307-1363
23.	a	UCIAMS-240425	RAS_DM2	Cape Rasmussen[1]	-65.2471	-64.0812	-24.8	1470 ± 15	1324	1300-1354

24.	a	UCIAMS-240424	RAS_DM5	Cape Rasmussen[1]	-65.2468	-64.0809	-24.0	1535 ± 15	1367	1315-1410
25.	a	UCIAMS-240422	CHA_DM4	Charles Point[1]	-64.2375	-60.993	-23.8	590 ± 15	545	525-623
26.	a	UCIAMS-240423	CHA_DM5	Charles Point[1]	-64.2374	-60.9928	-24.5	625 ± 15	608	545-630
*	a	UCIAMS-240421	CHA_DM3	Charles Point[1]	-64.2369	-60.9947	-26.5	1.0666 ± 0.0015 FM		modern
27.	a	UCIAMS-240450	COP_DM12	Robert Island[1]	-62.3784	-59.6651	-23.9	245 ± 15	188	151-298
28.	a	UCIAMS-240439	COP_DM6	Robert Island[1]	-62.3784	-59.6653	-22.5	225 ± 15	191	146-285
29.	a	UCIAMS-240449	COP_DM11	Robert Island[1]	-62.3783	-59.6652	-23.5	255 ± 15	204	151-303
30.	a	UCIAMS-240442	COP_DM9	Robert Island[1]	-62.3783	-59.6651	-24.2	265 ± 15	288	152-308
31.	a	UCIAMS-240441	COP_DM8	Robert Island[1]	-62.3783	-59.6652	-25.1	230 ± 15	190	148-286
32.	a	UCIAMS-240445	COP_DM5	Robert Island[1]	-62.3777	-59.6799	-22.3	210 ± 15	196	142-283
33.	a	UCIAMS-240444	COP_DM15	Robert Island[1]	-62.3775	-59.6668	-23.8	165 ± 15	106	0-268
34.	a	UCIAMS-240443	COP_DM13	Robert Island[1]	-62.3774	-59.6667	-24.0	215 ± 15	194	144-283
35.	a	UCIAMS-240440	COP_DM14	Robert Island[1]	-62.3774	-59.6668	-23.2	180 ± 15	152	0-278
36.	a	UCIAMS-240451	COP_DM4	Robert Island[1]	-62.3774	-59.6801	-22.4	215 ± 15	194	144-283
37.	a	UCIAMS-240446	COP_DM3	Robert Island[1]	-62.3771	-59.6806	-22.7	160 ± 15	102	0-264
38.	a	UCIAMS-240447	COP2_DM1	Robert Island[1]	-62.3746	-59.6735	-22.2	160 ± 15	102	0-264
39.	a	UCIAMS-240448	COP2_DM3	Robert Island[1]	-62.3744	-59.6732	-23.8	245 ± 15	188	151-298
40.	e	CAMS-170215	BON-DM-3	Anvers Island[3]	-64.7783	-64.0429		670 ± 25	604	554-654
41.	e	CAMS-170214	BON-DM-2	Anvers Island[3]	-64.7783	-64.0428		660 ± 35	605	549-655
42.	e	CAMS-170216	BON-DM-4	Anvers Island[3]	-64.7772	-64.0418		685 ± 25	602	556-660
43.	e	CAMS-170213	BON-DM-1	Anvers Island[3]	-64.7765	-64.0392		845 ± 25	707	672-764
44.	e	CAMS-170218	BON-DM-6	Anvers Island[3]	-64.7764	-64.0389		880 ± 25	742	681-794
45.	e	CAMS-170220	BON-DM-8	Anvers Island[3]	-64.7765	-64.0388		920 ± 25	773	727-901
46.	e	CAMS-170219	BON-DM-7	Anvers Island[3]	-64.7764	-64.0389		945 ± 25	803	736-905
47.	c	OS-57859	Site-1A	Norsel Pt. (Anvers Island)[5]				930 ± 30	785	728-905
48.	c	OS-57893	Site-2E	Norsel Pt. (Anvers Island)[5]				790 ± 30	685	575-730
49.	c	OS-57773	Site-3D	Norsel Pt. (Anvers Island)[5]				1050 ± 35	913	800-962

50.	c	OS-57860	Site-4A	Norsel Pt. (Anvers Island) [5]			860 ± 30	723	674-788
51.	c	OS-57894	Site-5C	Norsel Pt. (Anvers Island)[5]			820 ± 30	702	665-735
52.	c	OS-57895	Site-6	Norsel Pt. (Anvers Island)[5]			895 ± 35	756	680-898
53.	d	Beta-260750	Rothera3	Adelaide Island[4]	-67.5666	-68.11666	340 ± 40	386	290-486
54.	d	Beta-266189	Roth2009-1	Adelaide Island[4]	-67.5666	-68.11666	670 ± 40	605	550-660
55.	d	Beta-356172	M11	Adelaide Island[4]	-67.5666	-68.11666	540 ± 40	525	493-622
56.	b	AA-43571	ValleKlotz2	King George Island[6]			1453 ± 38	1313	1183-1374
57.	b	AA-46811	ValleKlotz3	King George Island[6]			1403 ± 41	1277	1177-1347
58.	b	AA-44275	ValleKlotz4	King George Island[6]			1338 ± 42	1220	1088-1298
59.	b	AA-43750	ValleKlotz5	King George Island[6]			1116 ± 48	979	819-1176
60.	b	AA-44277	ValleNorte17	King George Island[6]			1258 ± 37	1126	996-1264
61.	b	AA-44277	ValleNorte18	King George Island[6]			894 ± 41	757	675-903
62.	b	AA-44277	ValleNorte19	King George Island[6]			855 ± 32	718	672-787
63.	b	AA-44277	ValleNorte20	King George Island[6]			713 ± 37	616	557-673
64.	b	AA-44277	ValleNorte21	King George Island[6]			677 ± 45	605	549-664
65.	b	AA-44276	ValleNorte22	King George Island[6]			264 ± 37	222	141-440
66.	b	AA-46799	ValleNorte23	King George Island[6]			131 ± 31	92	0-258
67.	e	CAMS-170221	GAL-DM1	Galindez Island[3]			895 ± 25	755	684-799

Table S2. Radiocarbon dates (<2050 ^{14}C age) reflecting penguin colony abandonment used for the sum probability distribution. Published penguin dates used to summarize penguin colony abandonment on the western Antarctic Peninsula include remains such as bone, egg membrane, feather, squid beak collected from surfaces to 45 cm depth. The species include *Pygoscelis papua, P. adeliae, P. antarctica,* and *Pyschroteuthis* from a) (Emslie, 1995, 2001); b) (Emslie et al., 1998; Emslie, 2001); c) (Emslie, 2001); d) (Emslie et al., 2003); e) (Emslie et al., 2011); f) (Emslie et al., 2013); g) (Emslie et al., 2018); h) (Emslie et al., 2020); i) (Kalvakaalva et al., 2020);

ID	Source	Lab ID	Site	Species	Sediment level	Age (^{14}C yr BP)	Error (SD)	Median age (cal yr BP)	2-σ max	2-σ min
1	f	UGAMS 8853	Ardley Island	*P. papua*	3	1450	25	204	370	3
2	f	UGAMS 8852	Ardley Island	*P. papua*	4	1250	25	Invalid		
3	f	UGAMS 8685	Ardley Island	*P. papua*	6	1450	25	204	370	3
4	f	UGAMS 8684	Ardley Island	*P. papua*	7	1560	25	326	480	143
5	f	UGAMS 8682	Ardley Island	*P. papua*	8	2050	25	740	909	596
6	f	UGAMS 8683	Ardley Island	*P. papua*	8	1690	25	435	569	273
7	f	UGAMS 8687	Ardley Island	*P. papua*	bottom	1530	25	295	466	110
8	f	UGAMS 8688	Ardley Island	*P. papua*	bottom	1570	25	336	485	151
9	b	CAMS 42378	Biscoe Point	*P. adeliae*	1	1460	50	215	401	9
10	b	CAMS 42007	Biscoe Point	*P. adeliae*	1	1540	50	303	483	99
11	b	CAMS 42370	Biscoe Point	*P. adeliae*	1	1530	50	293	476	87
12	b	CAMS 42371	Biscoe Point	*P. adeliae*	2	1790	40	523	665	356
13	b	CAMS 42377	Biscoe Point	*P. adeliae*	1	1650	50	399	559	216
14	b	CAMS 42379	Biscoe Point	*P. adeliae*	1	1460	50	215	401	9
15	b	CAMS 42372	Biscoe Point	*P. adeliae*	1	1350	50	123	273	1
16	b	CAMS 42373	Biscoe Point	*P. adeliae*	1	1180	50	Invalid		
17	b	CAMS 42374	Biscoe Point	*P. adeliae*	2	1600	40	360	512	172
18	b	CAMS 42375	Biscoe Point	*P. adeliae*	2	1580	50	342	503	141
19	b	CAMS 42376	Biscoe Point	*P. adeliae*	3	1600	50	359	515	157

20	b	CAMS 38709	Biscoe Point	*Pyschroteuthis*	2	1580	50	342	503	141
21	b	CAMS 38708	Biscoe Point	*Pyschroteuthis*	3	1650	50	399	559	216
22	b	CAMS 42008	Cormorant Island	*Pygoscelis* sp.	2	1700	50	443	652	310
23	b	CAMS 42009	Cormorant Island	*Pygoscelis* sp.	2	1760	60	496	652	310
24	c	UA 1033	Devil Island	*P. adeliae*	0	1425	80	187	386	1
25	c	Beta 143249	Devil Island	*P. adeliae*	3	1480	40	236	428	41
26	c	Beta 141904	Ginger Island	*P. adeliae*	3	1090	40	Invalid		
27	c	Beta 141905	Ginger Island	*P. adeliae*	4	1580	50	342	503	141
28	c	Beta 141906	Ginger Island	*P. adeliae*	5	1770	40	506	648	335
29	c	Lu-3101	Hope Bay	*P. adeliae*	0	1280	50	Invalid		
30	g	OS-110720	Hope Bay	*P. adeliae*	1	1730	20	471	614	313
31	g	OS-110721	Hope Bay	*P. adeliae*	1	1460	20	214	400	30
32	g	OS-110722	Hope Bay	*P. adeliae*	1	1430	20	185	336	1
33	g	OS-110213	Hope Bay	*P. adeliae*	1	1340	20	109	252	1
34	g	OS-110214	Hope Bay	*P. adeliae*	2	1280	25	Invalid		
35	g	OS-110215	Hope Bay	*P. adeliae*	3	1370	25	133	272	1
36	g	OS-110216	Hope Bay	*P. adeliae*	1	1320	20	96	242	1
37	g	OS-110217	Hope Bay	*P. adeliae*	1	1480	25	237	424	51
38	g	OS-110218	Hope Bay	*P. adeliae*	2	1590	20	353	500	179
39	g	OS-110219	Hope Bay	*P. adeliae*	1	1460	20	214	400	30
40	g	OS-110221	Hope Bay	*P. adeliae*	1	1180	20	Invalid		
41	g	OS-110024	Hope Bay	*P. adeliae*	2	1270	20	Invalid		
42	g	OS-110222	Hope Bay	*P. adeliae*	1	1160	20	Invalid		
43	g	OS-110223	Hope Bay	*P. adeliae*	2	1240	20	Invalid		
44	g	OS-110224	Hope Bay	*P. adeliae*	1	1170	25	Invalid		
45	g	OS-110225	Hope Bay	*P. adeliae*	1	1120	20	Invalid		
46	g	OS-110025	Hope Bay	*P. adeliae*	1	1070	25	Invalid		
47	g	OS-110026	Hope Bay	*P. adeliae*	1	1100	20	Invalid		
48	b	CAMS 42006	Humble Island	*P. adeliae*	1	1160	50	Invalid		

49	b	CAMS 42003	Humble Island	*P. adeliae*	1	1400	50	161	322	1
50	b	CAMS 42004	Humble Island	*P. adeliae*	1	1360	40	127	273	1
51	b	CAMS 42005	Humble Island	*P. adeliae*	1	790	50	Invalid		
52	a	CAMS 15624	Blue Dyke, King George Island	*P. antarctica*	subsurface	1330	60	113	269	1
53	a	CAMS 14821	Blue Dyke, King George Island	*P. antarctica*	subsurface	1500	60	259	457	45
54	a	CAMS 14817	Low Head, King George Island	*P. antarctica*	0	1440	60	196	381	1
55	a	CAMS 15628	Uchatka, King George Island	*P.* cf. *P. antarctica*	2	1350	50	123	273	1
56	a	CAMS 15625	Uchatka, King George Island	*P. antarctica*	2	1380	60	147	310	1
57	a	CAMS 15629	Uchatka, King George Island	*P. antarctica*	1	1280	60	Invalid		
58	a	CAMS 15626	Uchatka, King George Island	*P.* cf. *P. antarctica*	1	1300	70	Invalid		
59	a	CAMS 15627	Low Head, King George Island	*P. antarctica*	0	1410	60	171	349	1
60	d	NZA 15416	Uchatka, King George Island	*P. antarctica*	4	1420	65	180	367	1
61	d	NZA 15417	Uchatka, King George Island	*P. antarctica*	5	1490	65	247	447	29
62	d	NZA 15418	Uchatka, King George Island	*P. antarctica*	3	1380	60	147	310	1
63	d	NZA 15419	Uchatka, King George Island	*P. antarctica*	4	1260	55	Invalid		
64	d	NZA 15414	Blue Dyke, King George Island	*P. antarctica*	3	1420	65	180	367	1
65	d	NZA 15415	Blue Dyke, King George Island	*P. antarctica*	4	1300	65	Invalid		
66	d	NZA 15412	Patelnia, King George Island	*P. antarctica*	5	1440	60	196	381	1
67	d	NZA 15413	Patelnia, King George Island	*P. antarctica*	5	1420	60	179	361	1
68	d	NZA 15406	Copa, King George Island	*P. papua*	1	1450	55	205	386	1
69	d	NZA 15539	Copa, King George Island	*P. papua*	2	1580	55	341	508	136
70	d	NZA 15407	Copa, King George Island	*P. papua*	3	1580	55	341	508	136
71	d	NZA 15408	Copa, King George Island	*Pygoscelis* sp.	4	1530	60	292	480	75
72	d	NZA 15409	Copa, King George Island	*Pygoscelis* sp.	4	1400	70	165	351	1
73	d	NZA 15410	Copa, King George Island	*P. adeliae*	2	1340	70	123	286	1
74	d	NZA 15411	Copa, King George Island	*P. papua*	2	740	55	Invalid		
75	d	NZA 15285	Rakusa Point, King George Island	*P. adeliae*	2	1380	65	148	318	1

76	d	NZA 15286	Rakusa Point, King George Island	*P. adeliae*	3	1500	55	259	455	50
77	d	NZA 15287	Rakusa Point, King George Island	*P. adeliae*	3	1430	60	187	372	1
78	d	NZA 15288	Rakusa Point, King George Island	*P. adeliae*	1	1410	55	170	343	1
79	d	NZA 15289	Rakusa Point, King George Island	*P. adeliae*	2	1370	65	141	306	1
80	d	NZA 15290	Rakusa Point, King George Island	*P. adeliae*	3	1500	65	258	459	41
81	d	NZA 15291	Rakusa Point, King George Island	*P. adeliae*	4	1490	60	248	446	34
82	d	NZA 15292	Rakusa Point, King George Island	*P. adeliae*	5	1670	60	416	605	242
83	d	NZA 15293	Rakusa Point, King George Island	*P. adeliae*	1	1480	65	236	431	17
84	d	NZA 15294	Rakusa Point, King George Island	*P. adeliae*	2	1360	55	131	285	1
85	d	NZA 15295	Rakusa Point, King George Island	*P. adeliae*	3	1450	60	206	390	1
86	d	NZA 15296	Rakusa Point, King George Island	*P. adeliae*	1	1290	55	Invalid		
87	d	NZA 15297	Rakusa Point, King George Island	*P. adeliae*	2	1480	65	236	431	17
88	d	NZA 15298	Rakusa Point, King George Island	*P. adeliae*	3	1310	65	105	262	1
89	d	NZA 15299	Rakusa Point, King George Island	*P. adeliae*	4	1340	55	118	271	1
90	d	NZA 15317	Rakusa Point, King George Island	*P. adeliae*	2	1530	55	292	478	81
91	d	NZA 15318	Rakusa Point, King George Island	*P. adeliae*	2	1450	55	205	386	1
92	h	OS-140164	Stranger Point, King George Island on Potter Peninsula	*Pygoscelis* sp.	1	1460	20	214	400	30

93	h	OS-140165	Stranger Point, King Goerge Island on Potter Peninsula	*Pygoscelis* sp.	2	1430	20	185	336	1
94	h	OS-140166	Stranger Point, King Goerge Island on Potter Peninsula	*Pygoscelis* sp.	3	1460	15	214	400	32
95	h	OS-140167	Stranger Point, King Goerge Island on Potter Peninsula	*Pygoscelis* sp.	5	1490	20	249	429	62
96	h	OS-140168	Stranger Point, King Goerge Island on Potter Peninsula	*Pygoscelis* sp.	7	1510	20	273	447	86
97	h	OS-140222	Stranger Point, King Goerge Island on Potter Peninsula	*Pygoscelis* sp.	9	1900	15	605	737	478
98	h	OS-140186	Stranger Point, King Goerge Island on Potter Peninsula	*Pygoscelis* sp.	10	1360	20	124	263	1
99	h	OS-140187	Stranger Point, King Goerge Island on Potter Peninsula	*Pygoscelis* sp.	12	1440	20	194	351	1
100	h	OS-140552	Stranger Point, King Goerge Island on Potter Peninsula	*Pygoscelis* sp.	14	1510	15	273	446	88
101	h	OS-140273	Stranger Point, King Goerge Island on Potter Peninsula	*Pygoscelis* sp.	16	1620	15	377	521	228
102	h	OS-140275	Stranger Point, King Goerge Island on Potter Peninsula	*Pygoscelis* sp.	1	1190	15	Invalid		
103	h	OS-140277	Stranger Point, King Goerge Island on Potter Peninsula	*Pygoscelis* sp.	2	1270	20	Invalid		
104	h	OS-140553	Stranger Point, King Goerge Island on Potter Peninsula	*Pygoscelis* sp.	5	1550	15	317	472	138
105	h	OS-140554	Stranger Point, King Goerge Island on Potter Peninsula	*Pygoscelis* sp.	6	1550	15	317	472	138
106	h	OS-140223	Stranger Point, King Goerge Island on Potter Peninsula	*Pygoscelis* sp.	n.a.	1440	20	194	351	1
107	f	UCIAMS 75543	Copa, King George Island	*P. papua*	2	1310	20	90	237	1
108	f	UCIAMS 75544	Copa, King George Island	*P. papua*	3	1330	20	102	247	1
109	a	CAMS 15644	Uchatka, King George Island	cf. *Pygoscelis* sp.	2	1340	60	119	275	1
110	a	CAMS 14609	Uchatka, King George Island	*Pygoscelis* sp.	3	1330	70	117	279	1
111	d	NZA 15613	Copa, King George Island	*Pygoscelis* sp.	3	1350	55	124	278	1

112	d	NZA 15614	Copa, King George Island	*Pygoscelis* sp.	3	1360	55	131	285	1
113	d	NZA 15612	Rakusa Point, King George Island	*P. adeliae*	5	1460	55	215	401	5
114	h	OS-140188	Stranger Point, King Goerge Island on Potter Peninsula	*Pygoscelis* sp.	8	1630	20	384	528	238
115	h	OS-140555	Stranger Point, King Goerge Island on Potter Peninsula	*Pygoscelis* sp.	n.a.	1610	15	369	513	212
116	c	Beta 141907	Lagoon Island	*Pygoscelis* sp.	2	1910	40	614	769	476
117	b	CAMS 42001	Litchfield Island	*P. adeliae*	1	1380	50	145	298	1
118	b	CAMS 42380	Litchfield Island	*P. adeliae*	1	1300	50	Invalid		
119	b	CAMS 42002	Litchfield Island	*P. adeliae*	2	1330	50	110	261	1
120	b	CAMS 41997	Litchfield Island	*P. adeliae*	1	1230	60	Invalid		
121	b	CAMS 41998	Litchfield Island	*P. adeliae*	2	1540	40	305	479	111
122	b	CAMS 41999	Litchfield Island	*P. adeliae*	1	1360	50	130	281	1
123	b	CAMS 42000	Litchfield Island	*P. adeliae*	2	1240	50	Invalid		
124	b	CAMS 42011	Litchfield Island	*P. adeliae*	3	1170	60	Invalid		
125	e	UCIAMS 59988	Byers Peninsula, Livingston Island	*Pygoscelis* sp.	1	1150	20	Invalid		
126	e	UCIAMS 59985	Byers Peninsula, Livingston Island	*Pygoscelis* sp.	6	1410	20	167	306	1
127	e	UCIAMS 59986	Byers Peninsula, Livingston Island	*Pygoscelis* sp.	7	1370	15	132	269	1
128	e	UCIAMS 59987	Byers Peninsula, Livingston Island	*Pygoscelis* sp.	8	1450	15	204	370	1
129	e	UCIAMS 59978	Byers Peninsula, Livingston Island	*Pygoscelis* sp.	2	1225	20	Invalid		
130	e	UCIAMS 59979	Byers Peninsula, Livingston Island	*Pygoscelis* sp.	4	1320	20	96	242	1
131	e	UCIAMS 59980	Byers Peninsula, Livingston Island	*Pygoscelis* sp.	2	1235	15	Invalid		
132	e	UCIAMS 68272	Byers Peninsula, Livingston Island	*Pygoscelis* sp.	2	1260	15	Invalid		

133	e	UCIAMS 9981	Byers Peninsula, Livingston Island	*Pygoscelis* sp.	3	1260	15	Invalid		
134	e	UCIAMS 59982	Byers Peninsula, Livingston Island	*Pygoscelis* sp.	4	1290	20	Invalid		
135	e	UCIAMS 68273	Byers Peninsula, Livingston Island	*Pygoscelis* sp.	4	1365	15	127	265	1
136	e	UCIAMS 60003	Byers Peninsula, Livingston Island	*Pygoscelis* sp.	1	1170	15	Invalid		
137	e	UCIAMS 60002	Byers Peninsula, Livingston Island	*Pygoscelis* sp.	1	1295	20	Invalid		
138	e	UCIAMS 59993	Byers Peninsula, Livingston Island	*Pygoscelis* sp.	3	1285	15	Invalid		
139	e	UCIAMS 59994	Byers Peninsula, Livingston Island	*Pygoscelis* sp.	4	1420	15	176	317	1
140	e	UCIAMS 59996	Byers Peninsula, Livingston Island	*Pygoscelis* sp.	5	1690	20	435	566	275
141	e	UCIAMS 59997	Byers Peninsula, Livingston Island	*Pygoscelis* sp.	1	1290	15	Invalid		
142	e	UCIAMS 59998	Byers Peninsula, Livingston Island	*Pygoscelis* sp.	5	1280	20	Invalid		
143	e	UCIAMS 59999	Byers Peninsula, Livingston Island	*Pygoscelis* sp.	7	1370	15	132	269	1
144	e	UCIAMS 60000	Byers Peninsula, Livingston Island	*Pygoscelis* sp.	8	1565	20	331	480	149
145	e	UCIAMS 60001	Byers Peninsula, Livingston Island	*Pygoscelis* sp.	8	1545	20	311	472	131
146	e	UCIAMS 75932	Byers Peninsula, Livingston Island	*Pygoscelis* sp.	n.a.	1445	20	199	358	1
147	a	CAMS14815	Penguin Island	*P.* cf. *P. adeliae*	0	1420	60	179	361	1
148	i	NOSAMS-145745	Platter Island, Danger Islands	*Pygoscelis* sp.	5	1690	15	436	563	277
149	a	CAMS14814	Seymour Island	*P.* cf. *P. adeliae*	0	1460	60	215	400	2
150	a	CAMS15623	Seymour Island	*P.* cf. *P. adeliae*	0	1490	60	248	446	34

151	g	OS-110212	Seymour Island	*P. adeliae*	bottom	925	20	Invalid		
152	g	OS-110023	Seymour Island	*P. adeliae*	bottom	765	20	Invalid		
153	b	CAMS 42010	Torgersen Island	*P. adeliae*	1	1190	40	Invalid		
154	b	CAMS 38710	Torgersen Island	*Psychroteuthis*	1	1280	50	Invalid		
155	i	NOSAMS-138692	Platter Island, Danger Islands	*Pygoscelis* sp.	1	885	15	Invalid		
156	i	NOSAMS-138696	Platter Island, Danger Islands	*Pygoscelis* sp.	2	1330	15	102	245	1
157	i	NOSAMS-138693	Platter Island, Danger Islands	*Pygoscelis* sp.	3	1560	15	327	477	146
158	i	NOSAMS-138694	Platter Island, Danger Islands	*Pygoscelis* sp.	4	1610	15	369	513	212

Table S3. ^{10}Be surface exposure ages in Lm scaling from James Ross Island (Kaplan et al., 2020) used in this study (Fig. 3B). Ages in Kaplan et al. 2020 were reported relative to the collection year (2014) and adjusted to the same scale as the black moss radiocarbon ages (relative to AD 1950).

Lab ID	Site	Context	Age	1-σ	cal BP
JRI-14-30	James Ross Island	ice edge/pond coverage?	100	10	36
JRI-14-43	James Ross Island	moraine (expanded)	100	10	36
JRI-14-29	James Ross Island	supraglacial debris/thrust ridge	120	10	56
JRI-14-42	James Ross Island	supraglacial debris/thrust ridge	180	20	116
JRI-14-50	James Ross Island	moraine (expanded)	220	20	156
JRI-14-28	James Ross Island	moraine (expanded)	230	10	166
JRI-14-27	James Ross Island	moraine (expanded)	310	20	246
JRI-14-41	James Ross Island	end of left lateral/ice edge	420	20	356
JRI-14-02	James Ross Island	moraine (expanded)	1440	70	1376

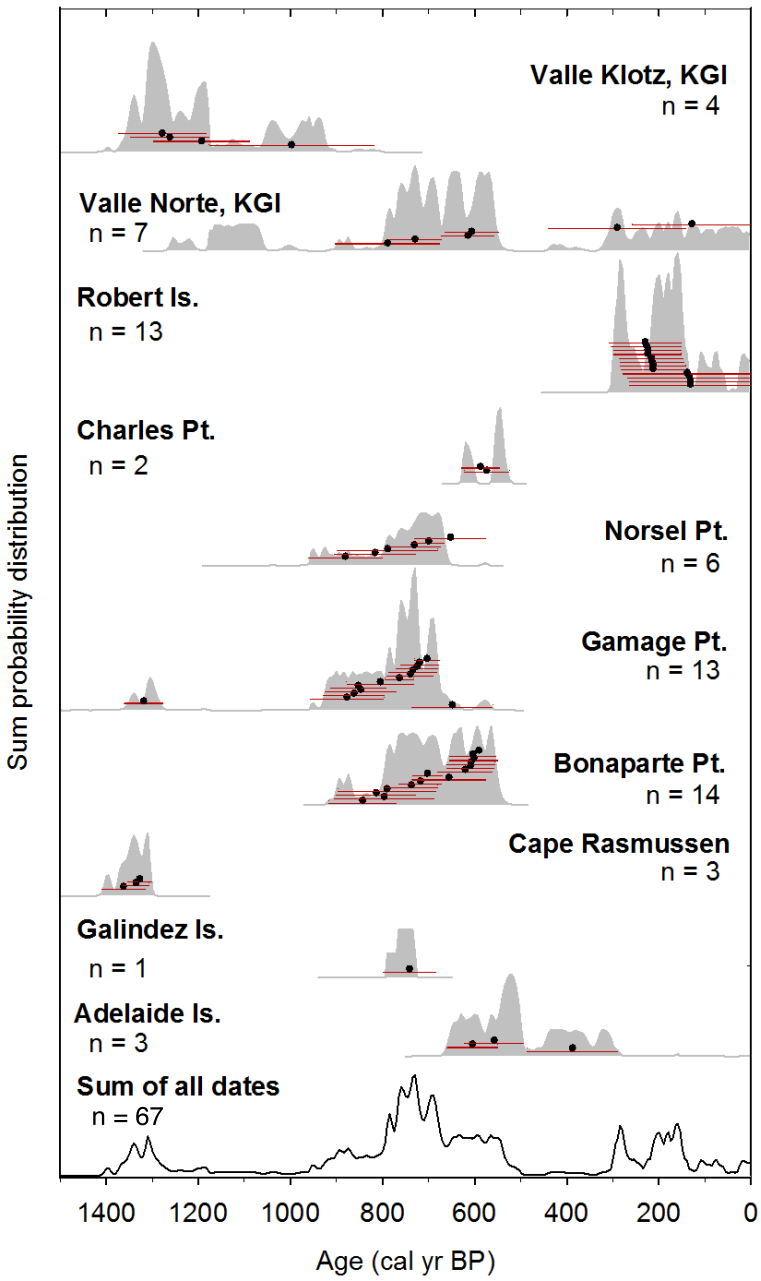

Figure S1. Antarctic Peninsula sum probability distributions of black moss calibrated radiocarbon dates from this study and published dates from Valle Klotz (n=4) and Valle Norte (n=7), King George Island and Norsel Point, Anvers Island (Hall, 2007, 2010), Bonaparte Point (n=7) and Galindez Island (n=1) (Yu et al., 2016), and Adelaide Island (Guglielmin et al., 2016) with median calibrated ages (black points) and 2-σ ranges (red bars) organized by latitude (north to south) over the past 1500 years.

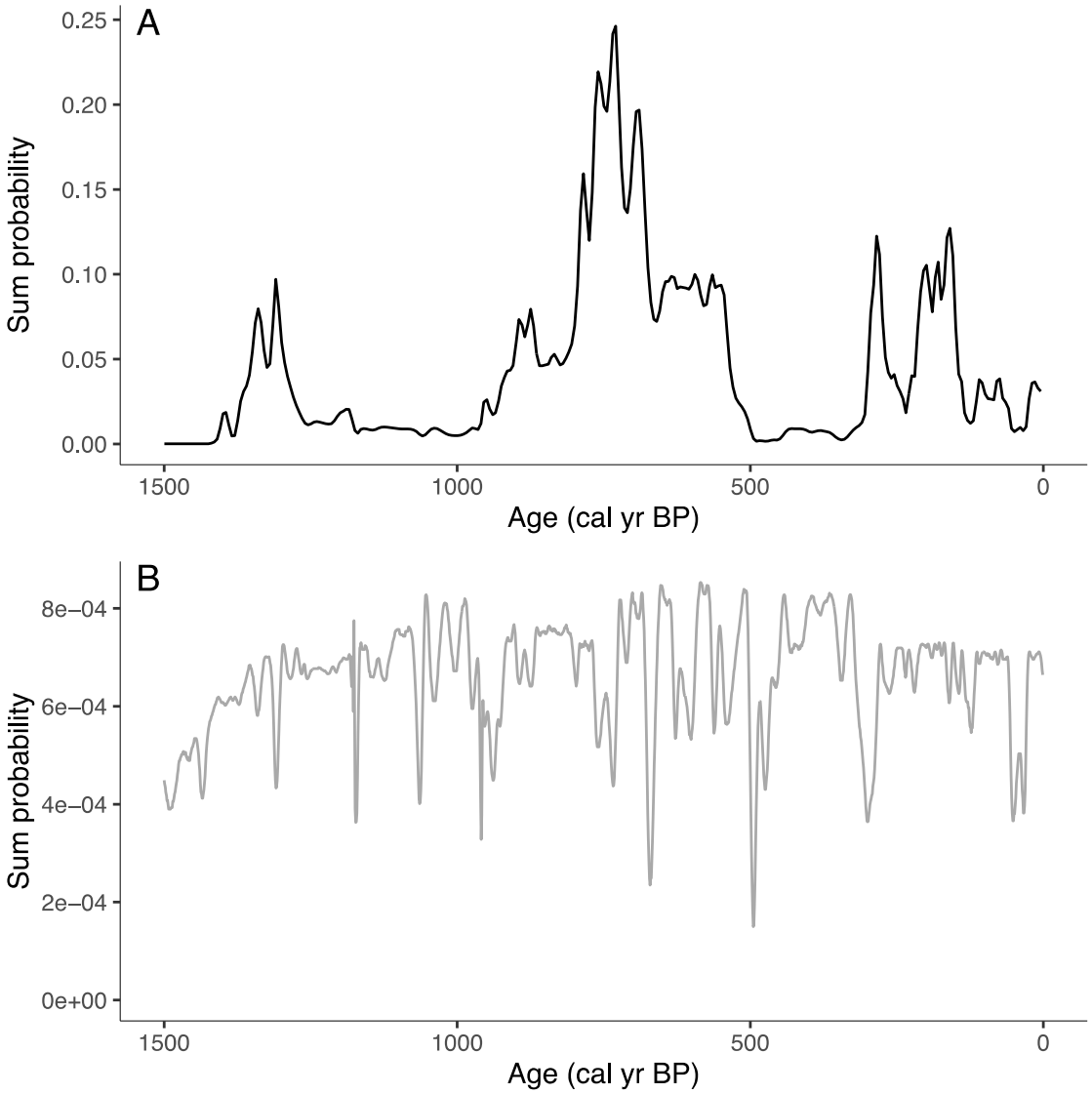

Figure S2. Sum probability distributions of moss kill dates and evenly spaced events to test for a calibration curve effect. A) Sum probability distribution of all published black moss calibrated radiocarbon dates (black line) and B) a curve of evenly spaced pseudo events every 22 years to detect the sensitivity of the calibration curve. The grey line represents the sum probability distribution of n=67 evenly spaced cal BP ages between 1500 and 0 ± 20 cal yr BP that were converted to ^{14}C year using the SHcal20 dataset (Hogg et al., 2020). The extracted ^{14}C ages were then calibrated using SHcal20.

SUPPLEMENTAL REFERENCES

Emslie, S.D., 1995, Age and taphonomy of abandoned penguin rookeries in the Antarctic Peninsula region: Polar Record, v. 31, p. 409–418, doi:10.1017/S0032247400027388.

Emslie, S.D., 2001, Radiocarbon dates from abandoned penguin colonies in the Antarctic Peninsula region: Antarctic Science, v. 13, p. 289–295, doi:10.1017/S0954102001000414.

Emslie, S.D., Baumann, K., and van Tuinen, M., 2011, Late Holocene occupation of Gentoo Penguins (Pygoscelis papua) on Byers Peninsula, Livingston Island, Antarctica: Polar Biology, v. 34, p. 283–290, doi:10.1007/s00300-010-0886-9.

Emslie, S.D., Fraser, W., Smith, R.C., and Walker, W., 1998, Abandoned penguin colonies and environmental change in the Palmer Station area, Anvers Island, Antarctic Peninsula: Antarctic Science, v. 10, p. 257–268, doi:10.1017/S0954102098000352.

Emslie, S.D., McKenzie, A., Marti, L.J., and Santos, M., 2018, Recent occupation by Adélie Penguins (Pygoscelis adeliae) at Hope Bay and Seymour Island and the 'northern enigma' in the Antarctic Peninsula: Polar Biology, v. 41, p. 71–77, doi:10.1007/s00300-017-2170-8.

Emslie, S.D., Polito, M.J., and Patterson, W.P., 2013, Stable isotope analysis of ancient and modern gentoo penguin egg membrane and the krill surplus hypothesis in Antarctica: Antarctic Science, v. 25, p. 213–218, doi:10.1017/S0954102012000740.

Emslie, S.D., Ritchie, P., and Lambert, D., 2003, Late-Holocene Penguin Occupation and Diet at King George Island Antarctic Peninsula, *in* Domack, E., Levente, A., Burnet, A., Bindschadler, R., Convey, P., and Kirby, M. eds., Antarctic Research Series, Washington, D. C., American Geophysical Union, p. 171–180, doi:10.1029/AR079p0171.

Emslie, S.D., Romero, M., Juáres, M.A., and Argota, M.R., 2020, Holocene occupation history of pygoscelid penguins at Stranger Point, King George (25 de Mayo) Island, northern Antarctic Peninsula: The Holocene, v. 30, p. 190–196, doi:10.1177/0959683619875814.

Guglielmin, M., Convey, P., Malfasi, F., and Cannone, N., 2016, Glacial fluctuations since the 'Medieval Warm Period' at Rothera Point (western Antarctic Peninsula): The Holocene, v. 26, p. 154–158, doi:10.1177/0959683615596827.

Hall, B.L., 2010, Holocene relative sea-level changes and ice fluctuations in the South Shetland Islands: Global and Planetary Change, v. 74, p. 15–26, doi:10.1016/j.gloplacha.2010.07.007.

Hall, B.L., 2007, Late-Holocene advance of the Collins Ice Cap, King George Island, South Shetland Islands: The Holocene, v. 17, p. 1253–1258, doi:10.1177/0959683607085132.

Hogg, A.G. et al., 2020, SHCal20 Southern Hemisphere Calibration, 0–55,000 Years cal BP: Radiocarbon, v. 62, p. 759–778, doi:10.1017/RDC.2020.59.

Kalvakaalva, R., Clucas, G., Herman, R.W., and Polito, M.J., 2020, Late Holocene variation in the Hard prey remains and stable isotope values of penguin and seal tissues from the Danger Islands, Antarctica: Polar Biology, v. 43, p. 1571–1582, doi:10.1007/s00300-020-02728-w.

Kaplan, M.R., Strelin, J.A., Schaefer, J.M., Peltier, C., Martini, M.A., Flores, E., Winckler, G., and Schwartz, R., 2020, Holocene glacier behavior around the northern Antarctic Peninsula and possible causes: Earth and Planetary Science Letters, v. 534, p. 116077, doi:10.1016/j.epsl.2020.116077.

La Farge, C., Williams, K.H., and England, J.H., 2013, Regeneration of Little Ice Age bryophytes emerging from a polar glacier with implications of totipotency in extreme environments: Proceedings of the National Academy of Sciences, v. 110, p. 9839–9844, doi:10.1073/pnas.1304199110.

Smith, R.I.L., 1982, Plant succession and re-exposed moss banks on a deglaciated headland in Arthur Harbour, Anvers Island.: British Antarctic Survey Bulletin, v. 51, p. 193–199.

Stuiver, M., and Reimer, P.J., 1993, Extended 14C Data Base and Revised CALIB 3.0 14C Age Calibration Program: Radiocarbon, v. 35, p. 215–230, doi:10.1017/S0033822200013904.

Yu, Z., Beilman, D.W., and Loisel, J., 2016, Transformations of landscape and peat-forming ecosystems in response to late Holocene climate change in the western Antarctic Peninsula: Geophysical Research Letters, v. 43, p. 7186–7195, doi:10.1002/2016GL069380.